Supporting Information:

Ferryl Protonation in Oxoiron(IV) Porphyrins and its Role in Oxygen Transfer

Nicholas C. Boaz, Seth R. Bell, and John T. Groves*

Department of Chemistry, Princeton University, Princeton New Jersey 08544, United States

jtgroves@princeton.edu. Telephone 609-258-3593

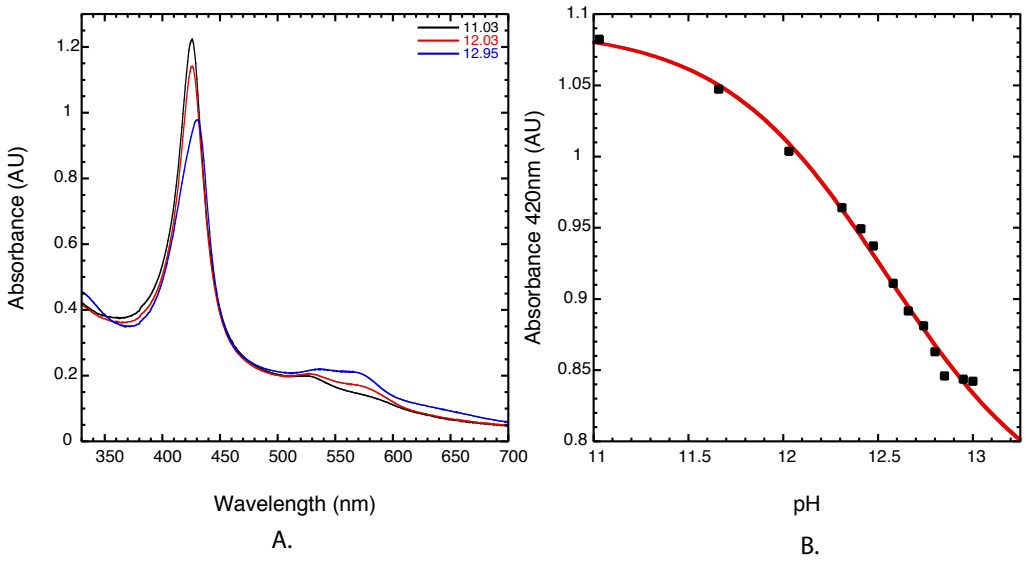

S1. (A.) UV-vis spectra of oxoFe^{IV}TMPS (12 μM) at pH 11-13 (unbuffered water). For higher pH regimes the Soret λ_{max} red-shifted from 425 nm (oxoaquaFe^{IV}TMPS shown in black) to a less intense band with a maximum at 431 nm (oxohydroxoFe^{IV}TMPS). (B.) Plot of absorbance at 420 nm versus pH revealed a pK_a at ~12.5.

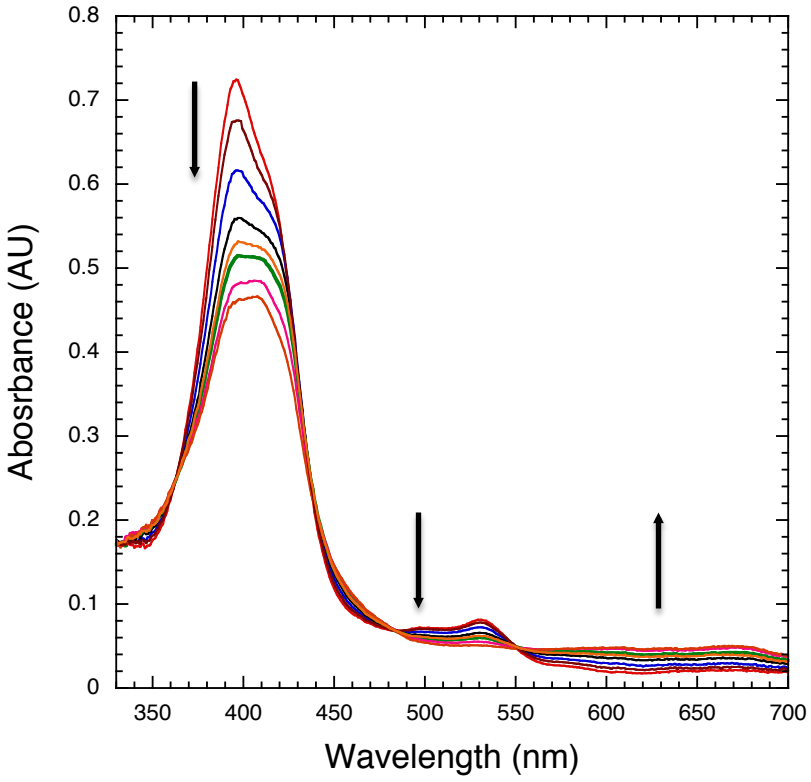

S2. Time-resolved spectra observed upon mixing FeTMPS (10 μM) with *m*CPBA (10 μM) at pH 5.4 (50 mM phosphate/acetate) resulting in the generation of oxoFe^{IV}TMPS^{+}. Selected traces shown for a 300 ms experiment. Concentrations presented are final concentrations after mixing.

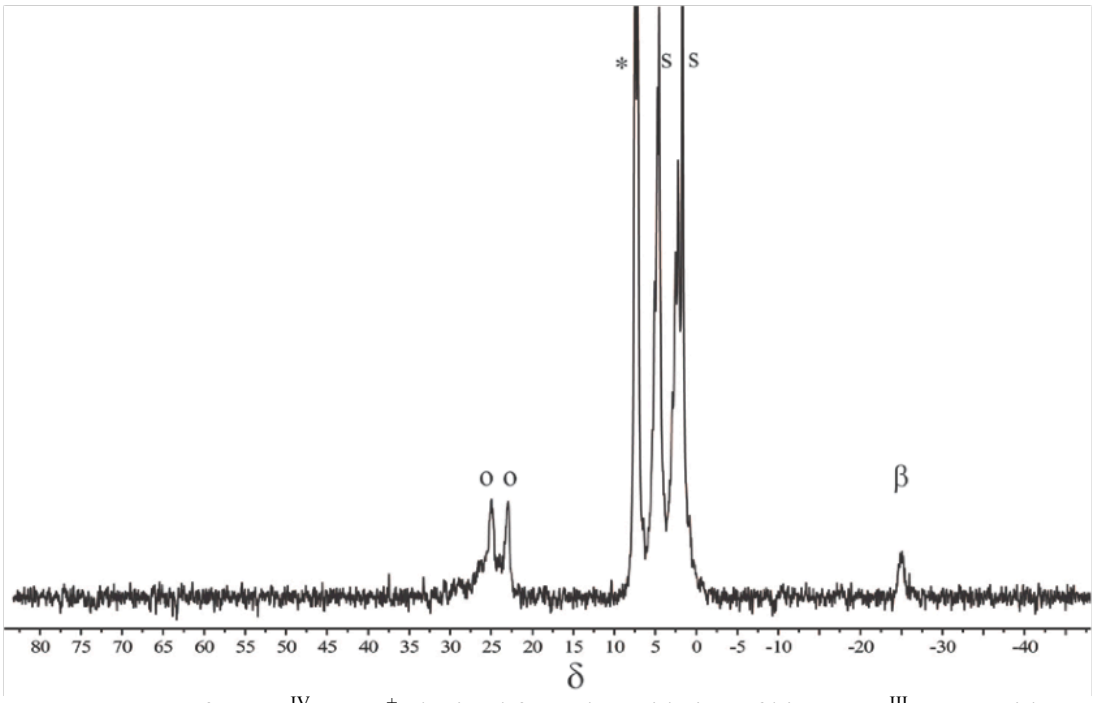

S3. ^{1}H NMR spectrum of oxoFe^{IV}TMPS^{+} obtained from the oxidation of bisaquaFe^{III}TMPS with *m*CPBA in 100 mM pD 5.05 deuterated acetic acid buffer at 5 ^{o}C; δ -26 (β-pyrrole) and δ 23, 25 (*o*-methyl), *m*CBA(*), and solvent (s).

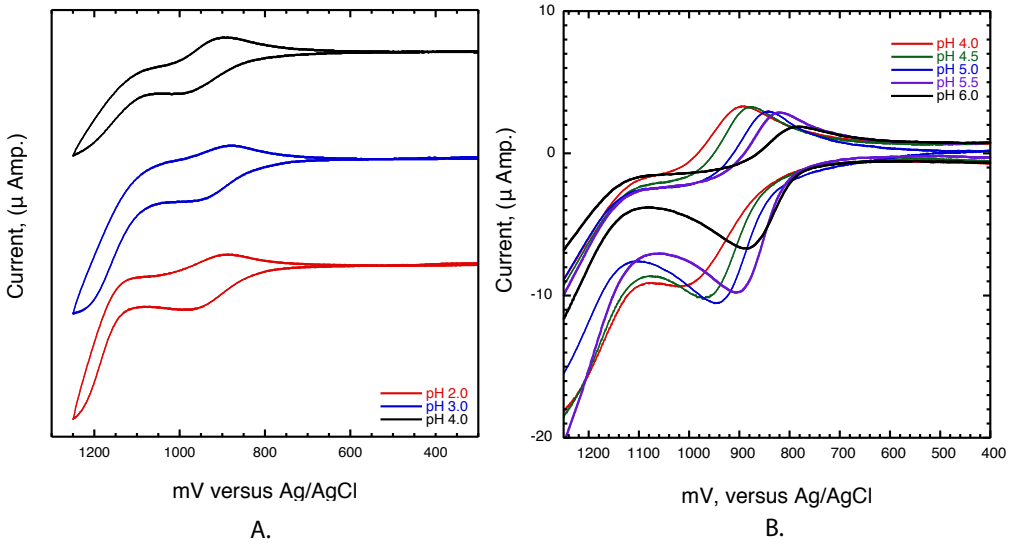

S4. (A). Cyclic voltammagrams of Fe^{III}TMPS at pH 2.0, 3.0 and 4.0. A pH independent wave was observed at 940 mV versus Ag/AgCl. (B.) Cyclic voltammagrams of Fe^{III}TMPS at pH 4.0, 4.5, 5.0, 5.5, and 6.0. At pH values greater than 4.0 the observed wave exhibited a pH dependence of -57 mV/pH unit. Fe^{III}TMPS (1 mM) in 100 mM buffer (phosphate/acetate) using a glassy carbon working electrode, platinum wire counter electrode, and Ag/AgCl reference electrode.

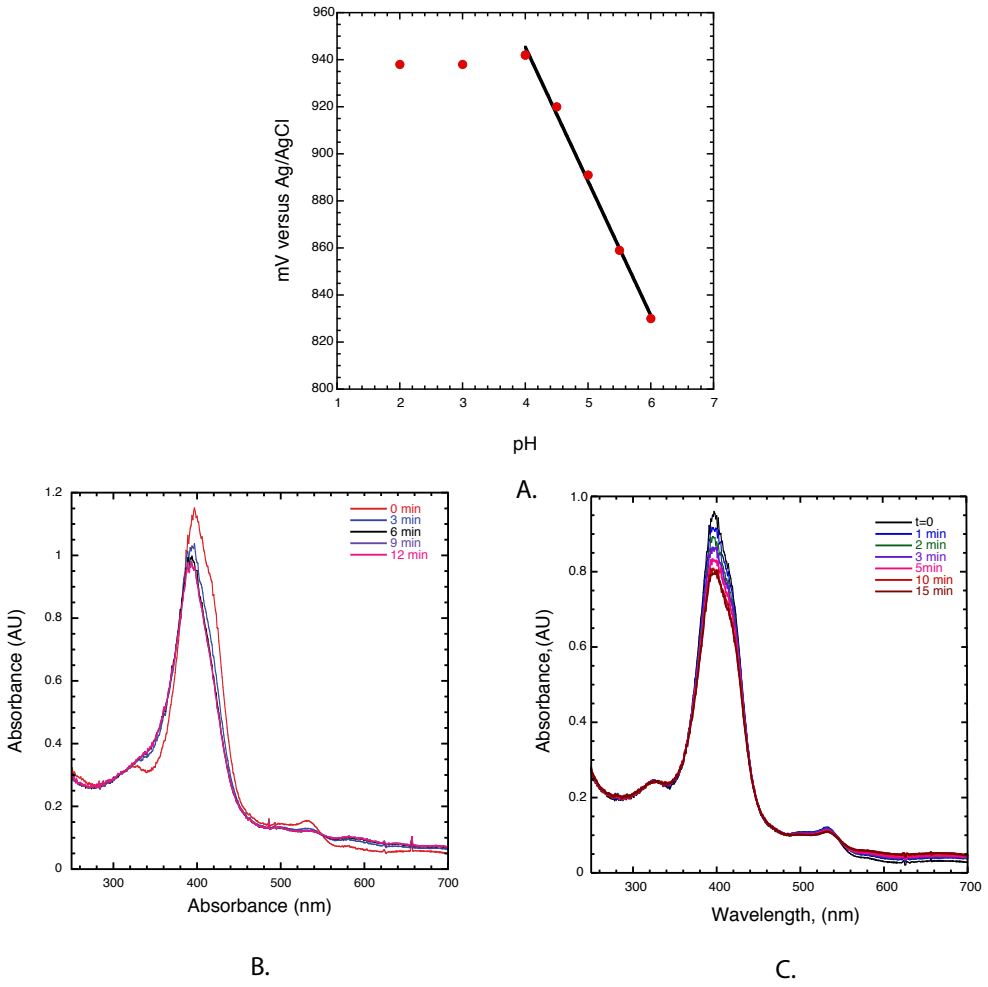

S5. (A) A Pourbaix plot of the CV redox waves shown in Figure S4B shows a pH independent component from pH 2.0 to pH 4.0. Above pH 4.0, the redox waves showed a slope of -57 mV/pH unit (R^2=0.99). (B) Spectroelectrochemical oxidation of 150 μM Fe^{III}TMPS at pH 2.0 (100 mM phosphate acetate buffer) over 12 min at 1100 mV yielded a new species with a Soret λ_{max} of 390 nm and an elevated Q-band feature at ~650 nm matching the spectrum of the previously reported $Fe^{III}TMPS^{+}$ derived from oxoFe^{IV}TMPS. [1] (C) Spectroelectrochemical oxidation of 150 μM Fe^{III}TMPS at pH 5.0 at 1200 mV vs Ag/AgCl yields an incomplete oxidation of Fe^{III}TMPS to oxoFe^{IV}TMPS. Spectroelectrochemical oxidation was performed in a 2 mm path length cuvette equipped with transparent platinum mesh working electrode, fritted platinum coil counter electrode, and Ag/AgCl reference electrode.

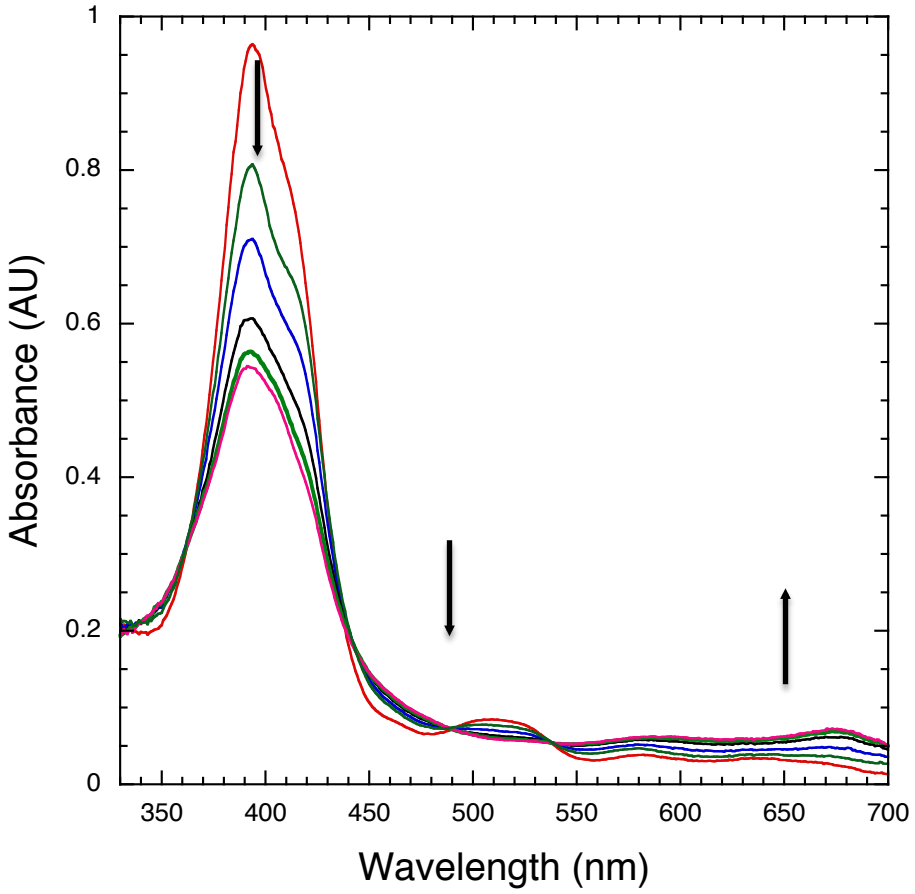

S6. Time-resolved spectra observed upon mixing FeTDClPS (10 μM) with *m*CPBA (10 μM) at pH 5.0 (50 mM phosphate/acetate) resulting in the generation of oxoFe^{IV}TDClPS^{+}. Selected traces shown for a 300 ms experiment. Concentrations presented are final concentrations after mixing.

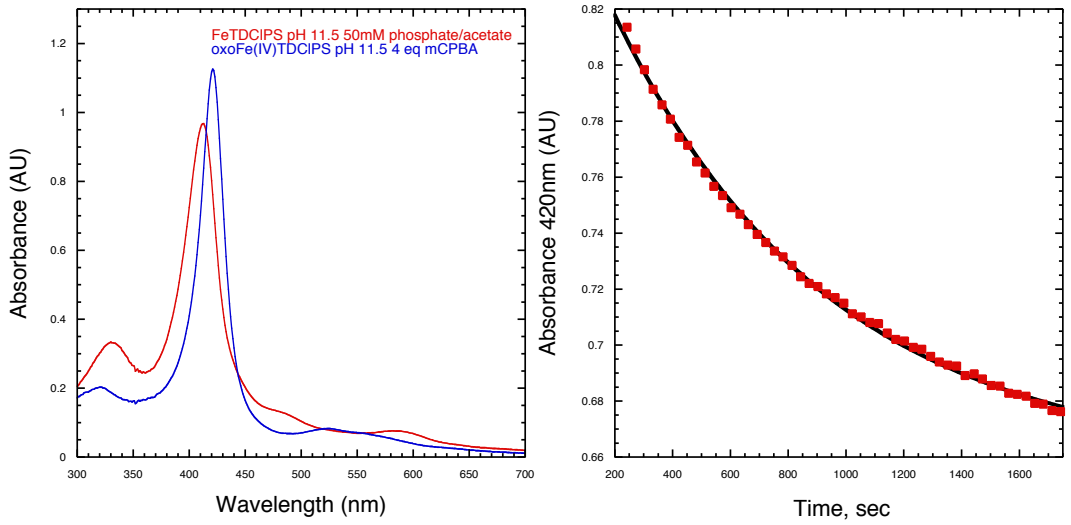

S7. (Left) Fe^{III}TDClPS (10 μM) at pH 11.5 (50 mM phosphate/acetate buffer). Treatment of Fe^{III}TDClPS with 4 eq of *m*CPBA resulted in the formation of a new species with a sharper, blue shifted Soret band at 420 nm. Upon comparison with FeTSMP and FeTMPS we assign this species as oxoFe(IV)TDClPS. (Right) The decay of $oxoFe^{IV}$ was measured by following the change in absorbance at 420 nm over time. Fitting these data to a single exponential equation (solid black line) resulted in a unimolecular decay rate constant of 0.00159 s^{-1}.

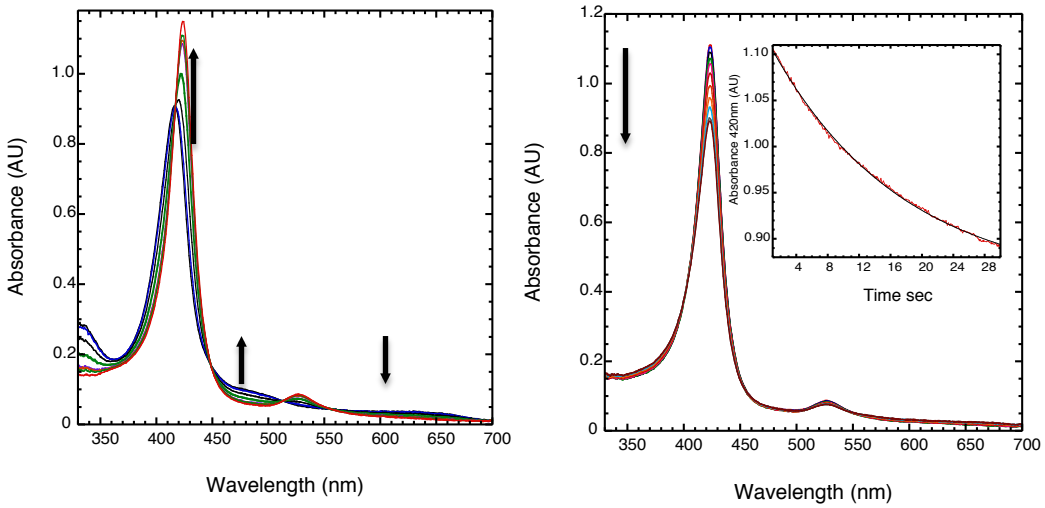

S8. (Left) Time-resolved spectra observed upon mixing FeTDPS (20 μM) with *m*CPBA (20 μM) at pH 11.5 (50 mM phosphate/acetate) to form oxoFe^{IV}TDPS, which displayed a sharpened, red-shifted Soret band at 423 nm. Selected traces shown for a 300 ms experiment where the authentic spectrum for oxoFe^{IV}TDPS was extracted using global fit analysis (red trace). (Right) Time resolved spectra of the spontaneous decay of oxoFe^{IV}TDPS over the course of 30 s (partial bleaching). (Inset) Fitting the decay at 420 nm for oxoFe^{IV}TDPS (red trace) to a single exponential function (black trace) afforded a rate constant of 0.059 ± 0.0007 s^{-1}.

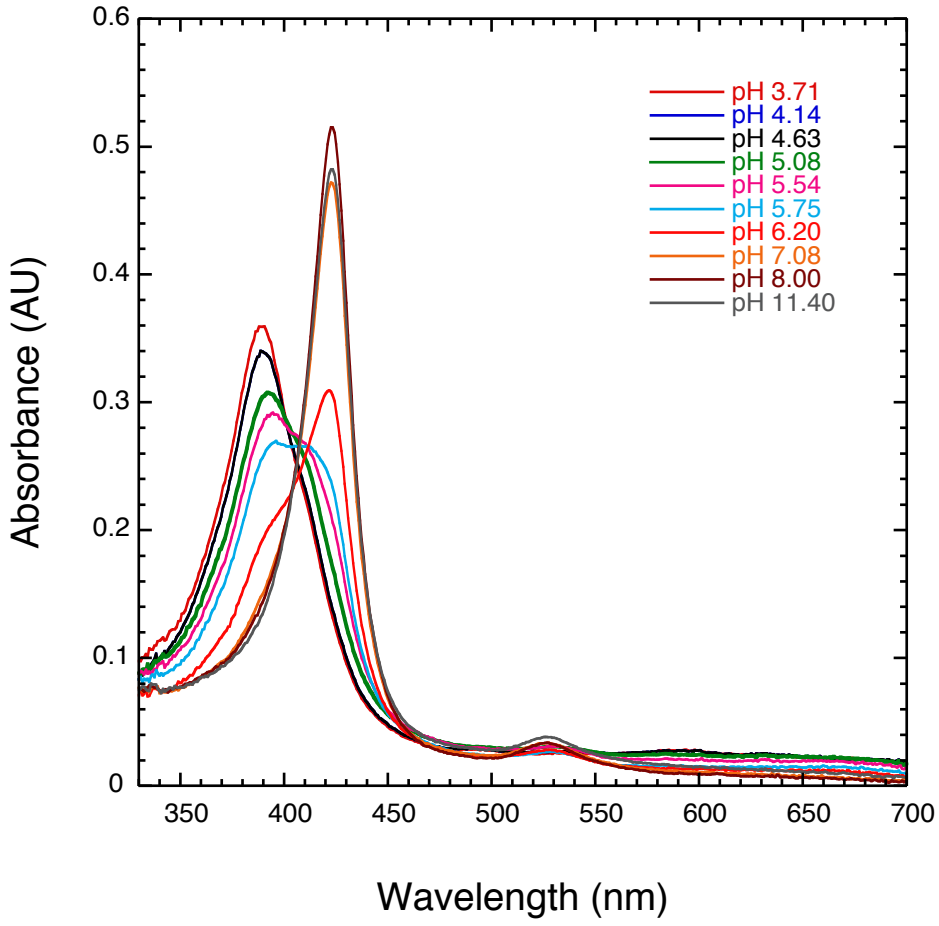

S9. UV-vis spectra observed within 10 ms after rapid dilution of oxoFe^{IV}TDPS (10 μM pH 11.5) with 50 mM phosphate/acetate buffer at the target pH (pH was measured after mixing). At high pH, ≥ 8.0, oxoFe^{IV}TDPS is observed, while at pH < 5 Fe^{III}TDPS^{+} was generated. At intermediate pH regimes, mixtures of oxoFe^{IV}TDPS and Fe^{III}TDPS^{+} were observed.

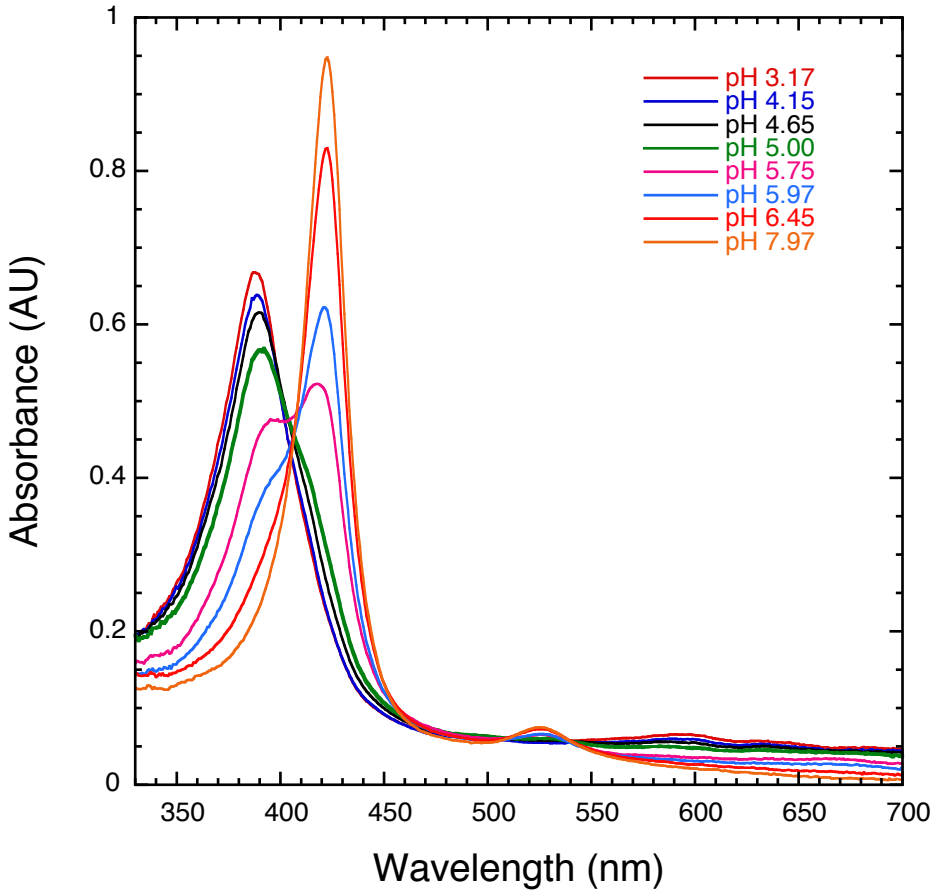

S10. UV-vis spectra observed within 10 ms after rapid dilution of oxoFe^{IV}TSMP (10 μM, pH 11.5) with 50 mM phosphate/acetate buffer at the target pH (pH was measured after mixing). At pH 7.97, oxoFe^{IV}TSMP was observed, while at pH < 4 Fe^{III}TSMP^{+} was generated. At intermediate pH regimes, mixtures of oxoFe^{IV}TSMP and Fe^{III}TSMP^{+} were observed.

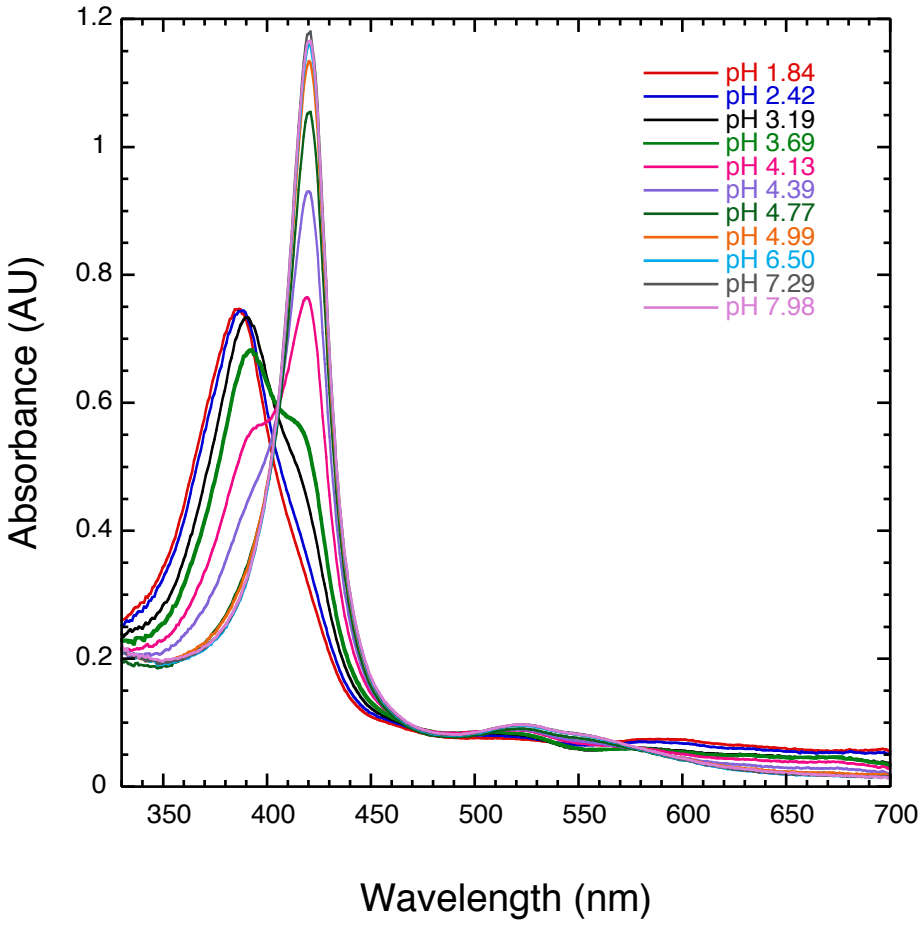

S11. UV-vis spectra observed within 10 ms after rapid dilution of oxoFe^{IV}TDClPS (10 μM, pH 11.5) with 50 mM phosphate/acetate buffer at the target pH (pH was measured after mixing). At pH > 7, oxoFe^{IV}TDClPS was observed, while at pH < 4 Fe^{III}TDClPS^{+} was generated. At intermediate pH regimes, mixtures of oxoFe^{IV}TDClPS and Fe^{III}TDClPS^{+} were observed.

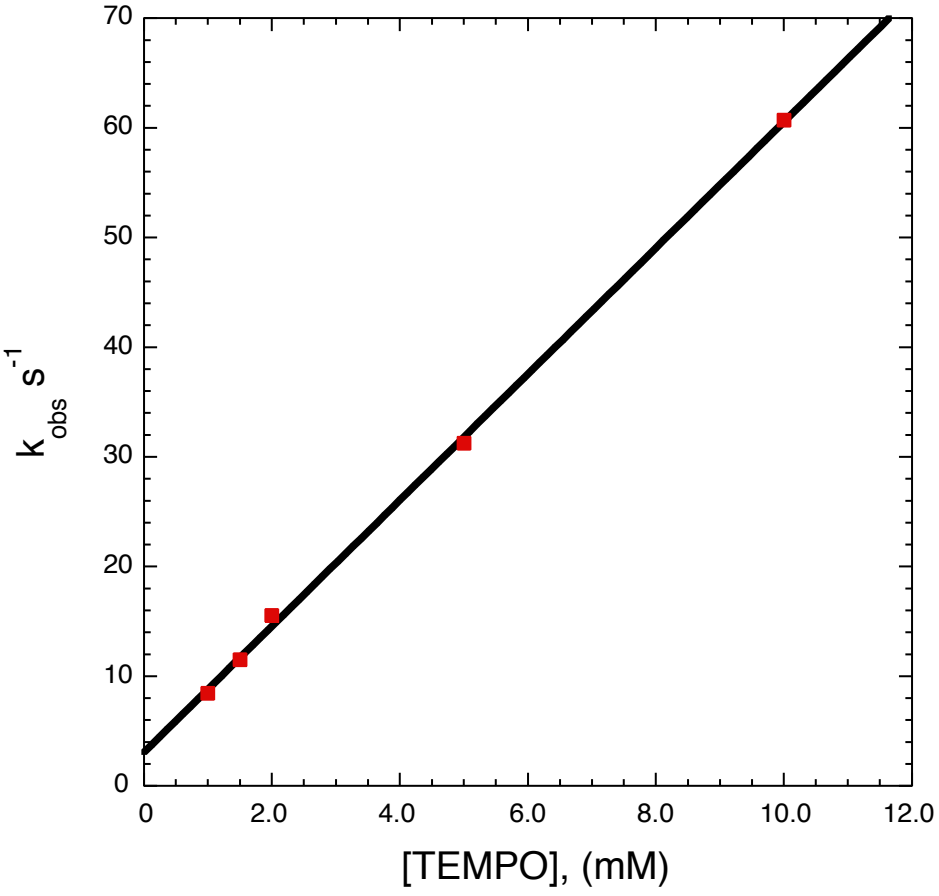

S12. Double-mixing stopped-flow experiment in which 20 μM oxoFe^{IV}TMPS was generated in the first push by stiochiometric oxidation with *m*CPBA. After a 30 s delay to ensure maximal generation of oxoFe^{IV}TMPS, TEMPO radical was added and the pseudo first-order rate constants, k_{obs}, were obtained by fitting the decrease in absorbance at 425 nm to a single exponential equation. Plotting k_{obs} versus the concentration of TEMPO added yielded a bimolecular rate constant of 5.75 $\pm$0.15 x 10^4 $M^{-1}s^{-1}$ (R^2=0.99). The reaction was performed at pH 8.0 in phosphate acetate buffer (50 mM) at 14.5°C. All concentrations presented are final concentrations after mixing.

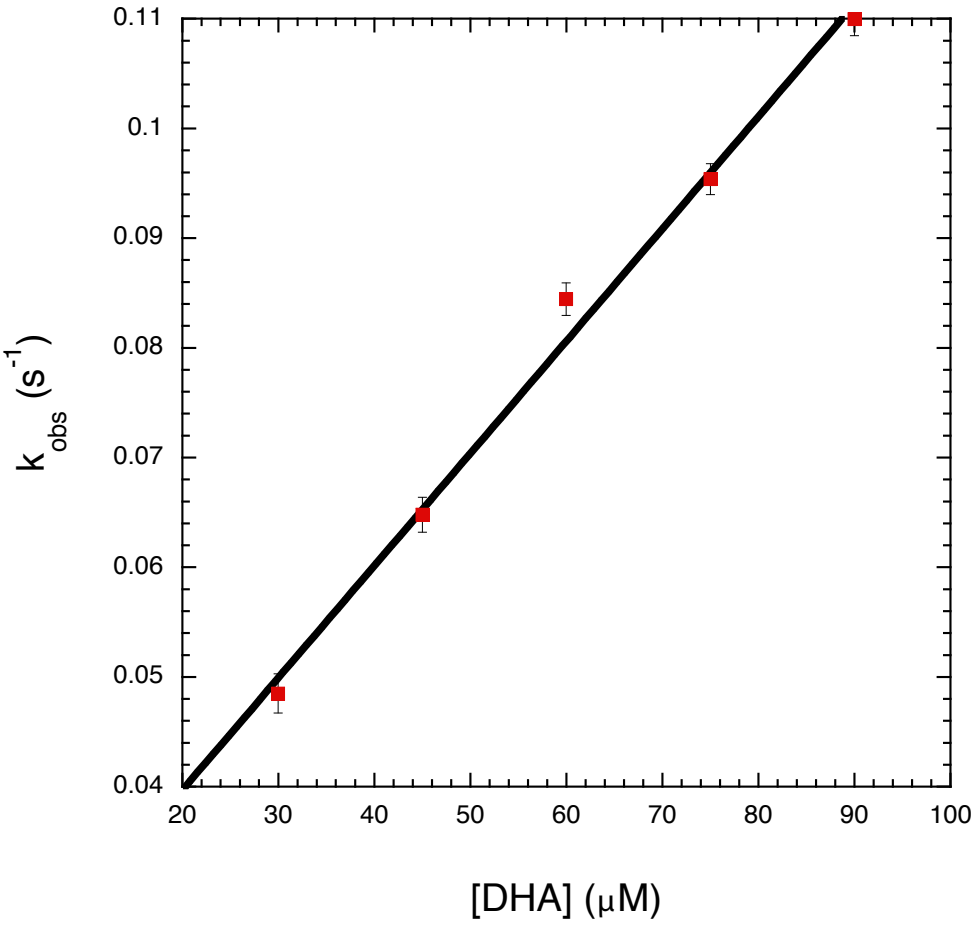

S13. Oxidation of dihydroanthracene (DHA) by oxoFe^{IV}TMPS^{+} in a double mixing, stopped flow experiment. In the first push, 3 μM Fe^{III}TMPS was treated with 1 equiv of *m*CPBA, generating oxoFe^{IV}TMPS^{+}. After a 2 s delay to ensure maximal generation, dihydroanthracene was introduced in a second push using 50 mM phosphate acetate buffer containing 20% acetonitrile at 14.5°C. Plotting concentration of DHA versus the observed rate constant for disappearance of oxoFe^{IV}TMPS^{+} yielded a bimolecular rate constant for DHA oxidation of 1023 ± 52 $M^{-1}S^{-1}$ (R^2=0.99). All concentrations presented are final after mixing.

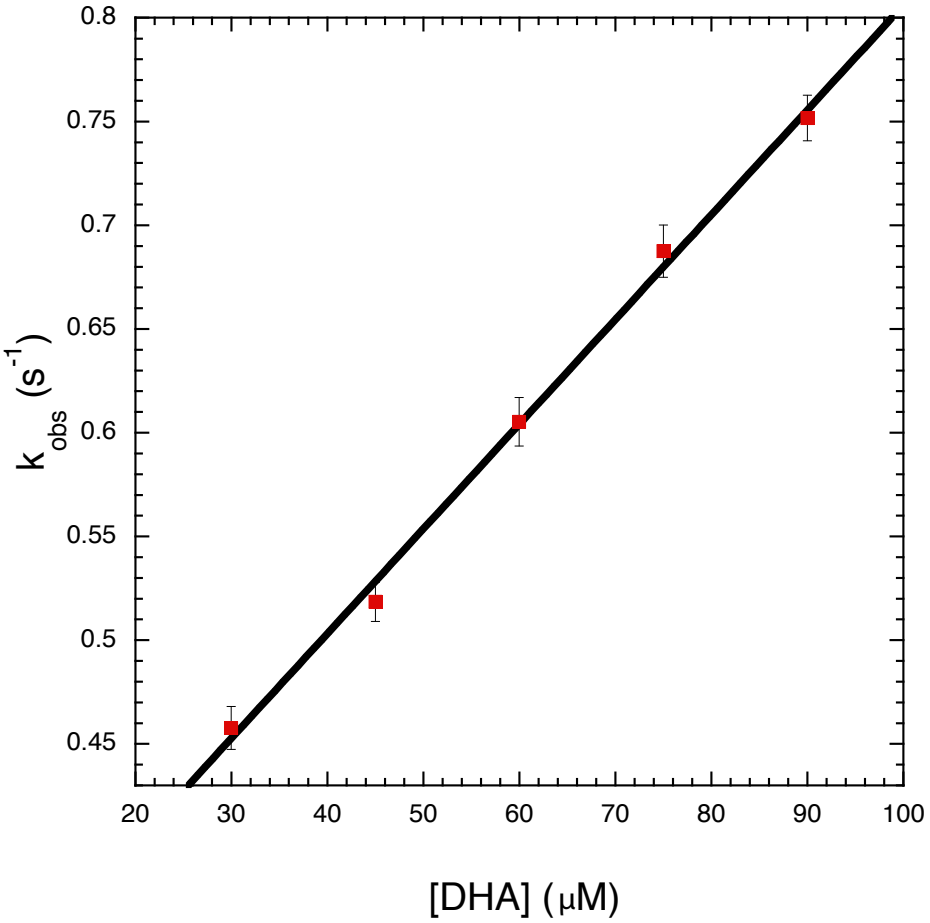

S14. Oxidation of DHA by oxoFe^{IV}TDClPS^{+} in a double-mixing stopped-flow experiment. In the first push, 3 μM Fe^{III}TDClPS was treated with 1 equiv of *m*CPBA generating oxoFe^{IV}TDClPS^{+}. After a 3 s delay to ensure maximal generation, DHA was introduced in a second push using 50 mM phosphate acetate buffer containing 20% acetonitrile at 14.5°C. Plotting concentration of DHA versus the observed rate constant for disappearance of oxoFe^{IV}TDClPS^{+} yielded a bimolecular rate constant for DHA oxidation of 5015 ± 170 $M^{-1}S^{-1}$ (R^2=0.99). All concentrations presented are final after mixing.

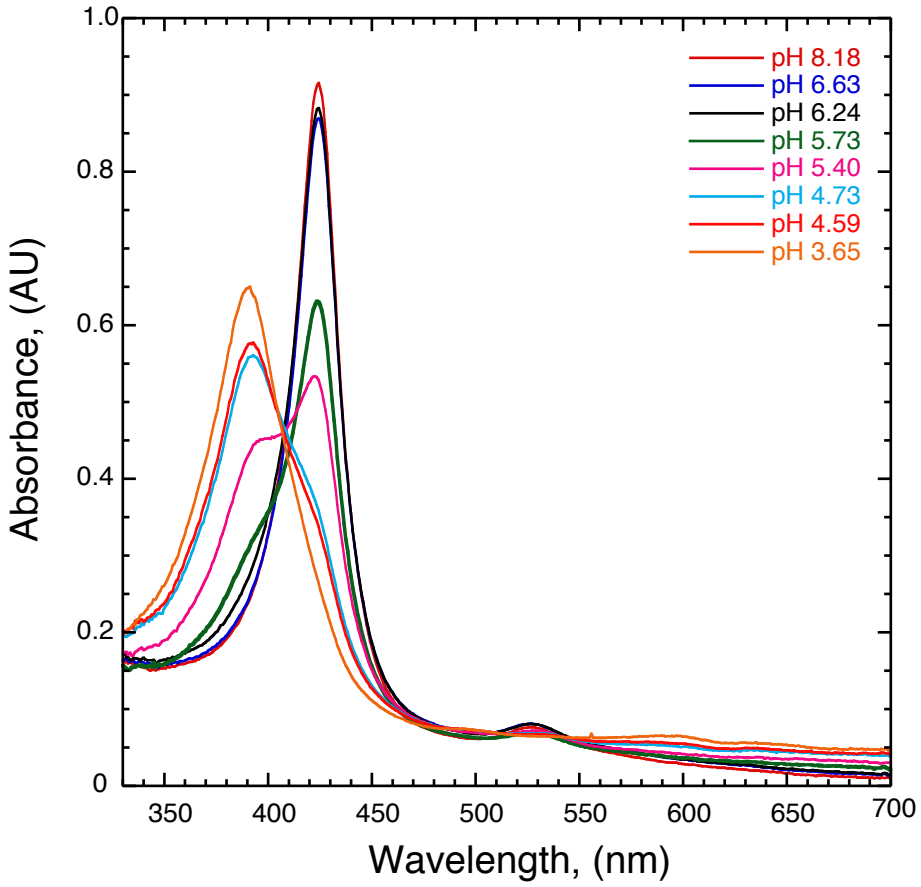

S15. UV-vis spectra produced by rapid pH jumping of oxoFe^{IV}TMPS (10 μM pH 11.5) with 50 mM phosphate/acetate buffer. Note the isosbestic conversion from oxoFe^{IV}TMPS at high pH to bisaquaFe^{III}TMPS porphyrin cation radical at low pH.

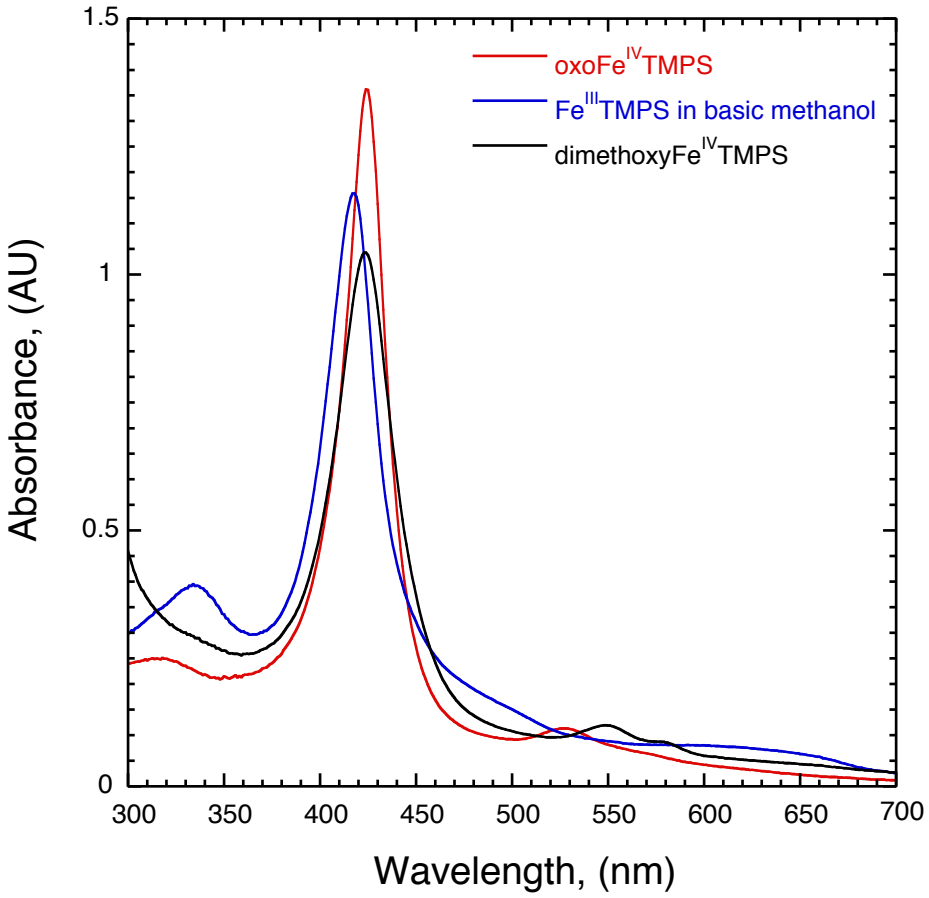

S16. UV-vis spectra of 10 μM Fe^{III}TMPS in basic methanol (50mM NaOH), 10 μM dimethoxyFe^{IV}TMPS and 10 μM oxoFe^{IV}TMPS at pH 11.5 in buffered water (50 mM phosphate acetate).[1]

SVD and EFA Analyses of pK_a^{obs} Data

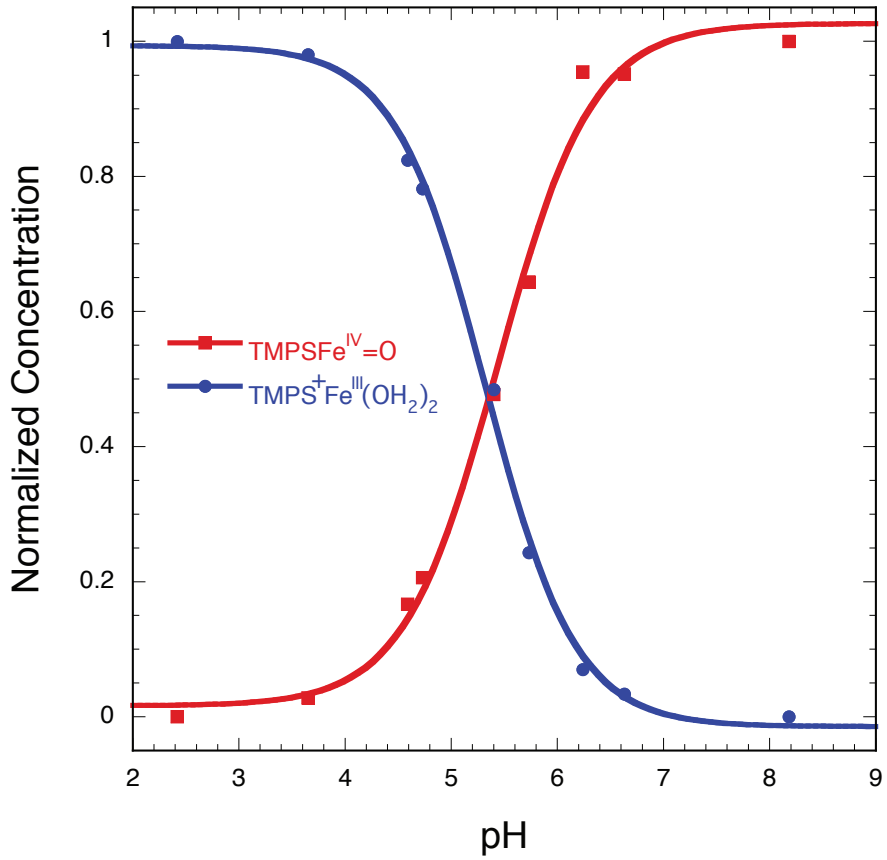

Figure S17. Concentration profile for the two observed electromers, $TMPSFe^{IV}=O$ and $TMPSFe^{III}(OH_2)_2$, as determined by model free evolving factor analysis (EFA) of the titration data shown in Figure S15. The pK_a^{obs} values determined by fitting the SVD speciation data are 5.32 ± 0.04 ($TMPSFe^{III}(OH_2)_2$ fit) and 5.44 ± 0.07 ($TMPSFe^{IV}=O$ fit).

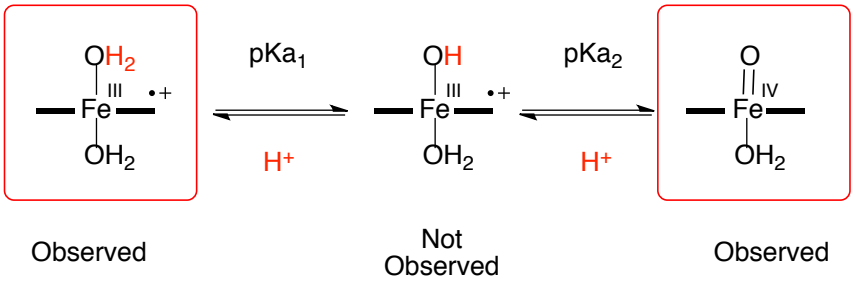

Scheme S1. Two state equilibrium model proposed for water-soluble compound II mimics.

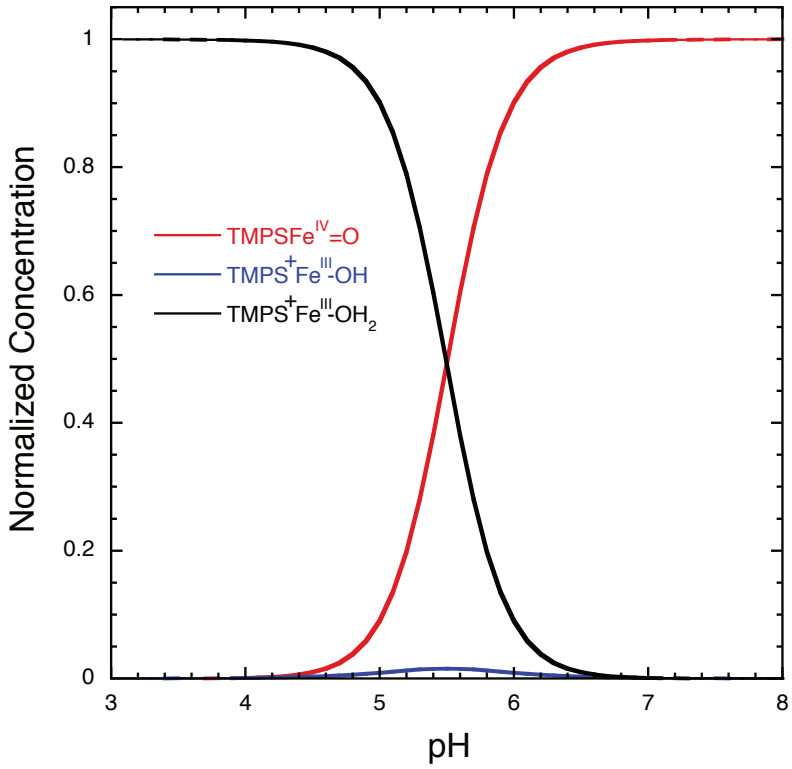

Figure S18. Modeled speciation plot for TMPS-II over a pH range of 3 to 8 using the equilibrium model shown in Scheme S1 with pK_a1=7 and pK_a2=4, assuming a two-proton equilibrium. Note the lack of appreciable buildup of the mono-protonated HO-Fe^{III}TMPS^{+} predicted by these pK_a values (< 1.6 % of total porphyrin species in solution).

$$Concentration = Con_{Max} + (Con_{Min}-Con_{Max})/ (1+ exp((pH-pKa_{obs}))/dx))$$

Equation S1. Boltzmann sigmoidal equation where Con_{Max}= the maximum observed concentration, Con_{Min} = the minimum observed concentration, and *dx* is the rate term for the change in concentration relative to the change in pH which can be used to ascertain the number of protons involved in the titration.

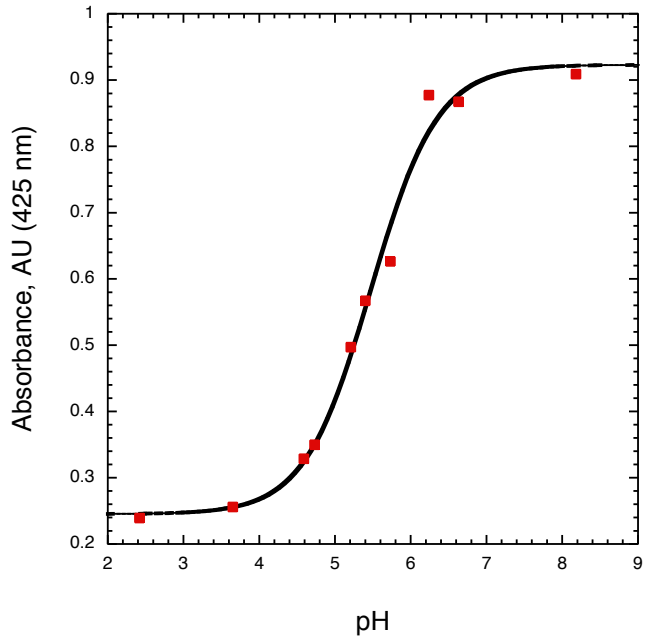

Figure S19. Boltzmann sigmoidal fit (eq S1) for the titration presented in Figure S15. Con_{Max}= 0.92 ± 0.03, Con_{Min}= 0.25 ± 0.3, pKa = 5.47 ± 0.08, and dx = 0.44 ± 0.07.

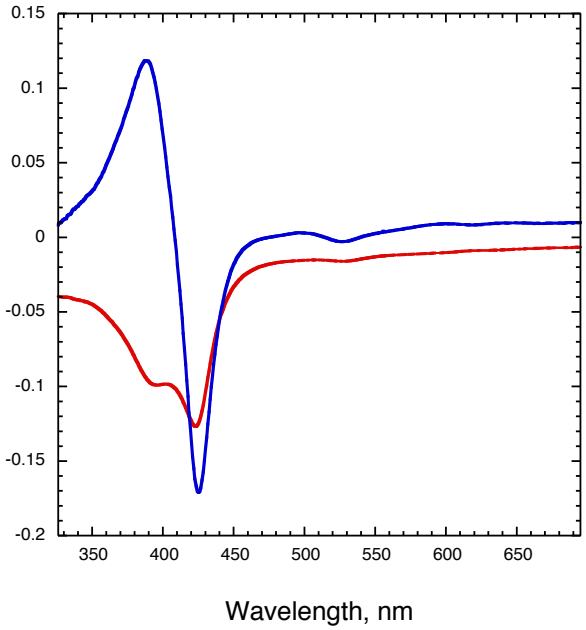

Figure S20. Abstract spectra resulting from the SVD analysis of the titration results of FeTMPS II in Figure S15. Only two significant non-zero singular values were obtained from SVD analysis.

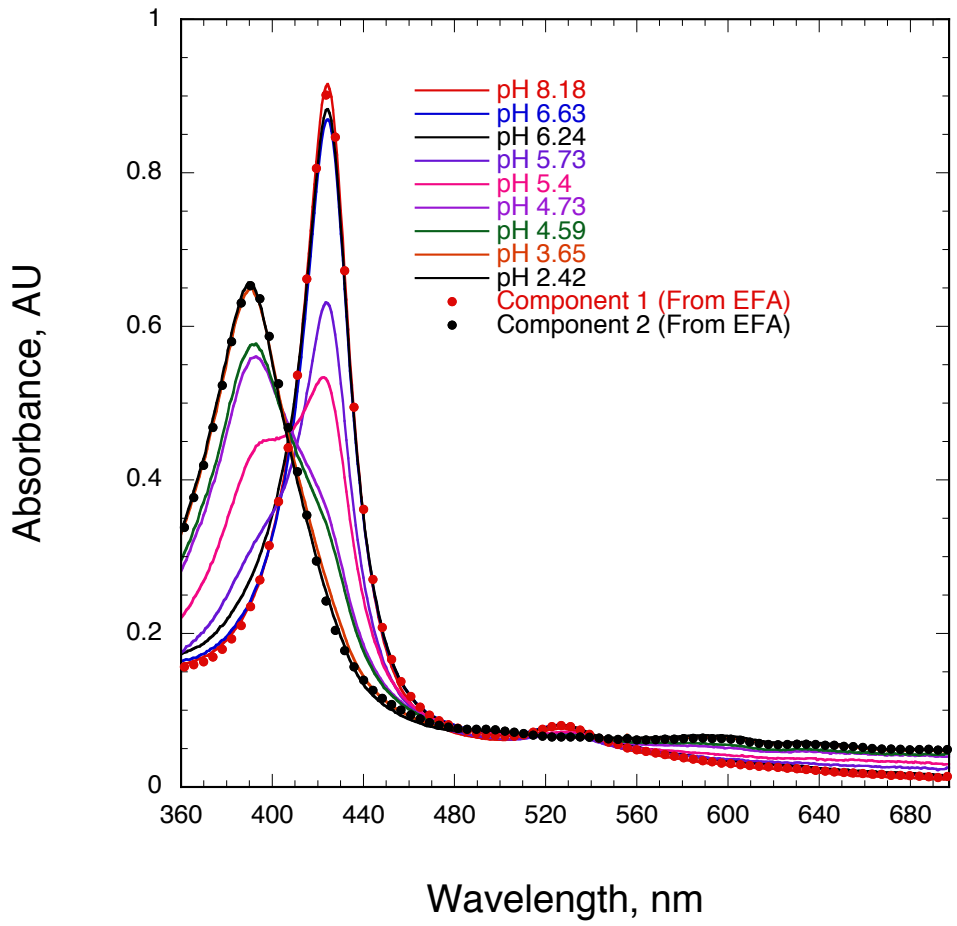

Figure S21. UV-vis spectra of the two components, $TMPSFe^{IV}=O$ and $TMPSFe^{III}(OH_2)_2$ (red and black dotted lines, respectively), reproduced using model free evolving factor analysis (EFA) of the titration data overlaid with the experimental titration data for FeTMPS-II.

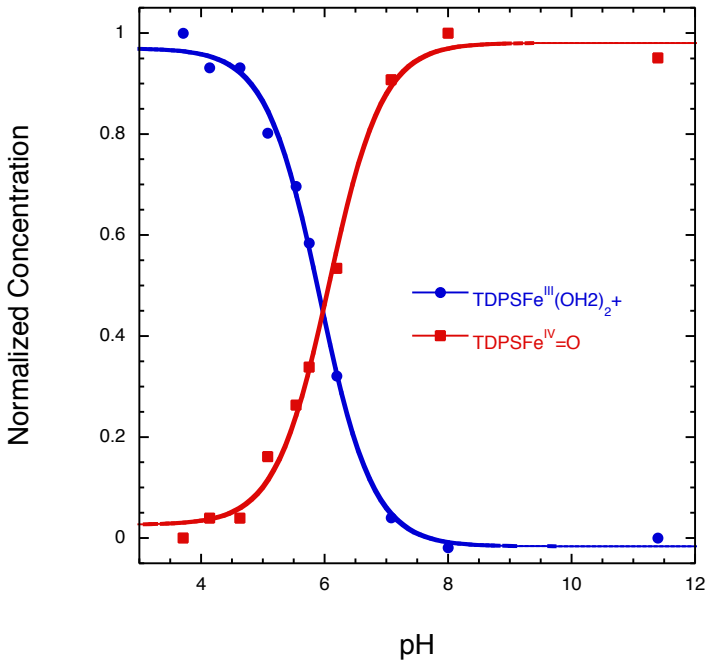

Figure S22. Concentration profile for the two observed electromers of FeTDPS-II as determined by model free evolving factor analysis (EFA) of the titration data shown in Figure S9. The observed pK_a^{obs} values determined by fitting the SVD speciation data are 5.92 ± 0.04 (TDPSFe^{III}(OH$_2$)$_2$ fit) and 6.07 ± 0.05 (TDPSFe^{IV}=O fit), dx = 0.50 ± 0.04.

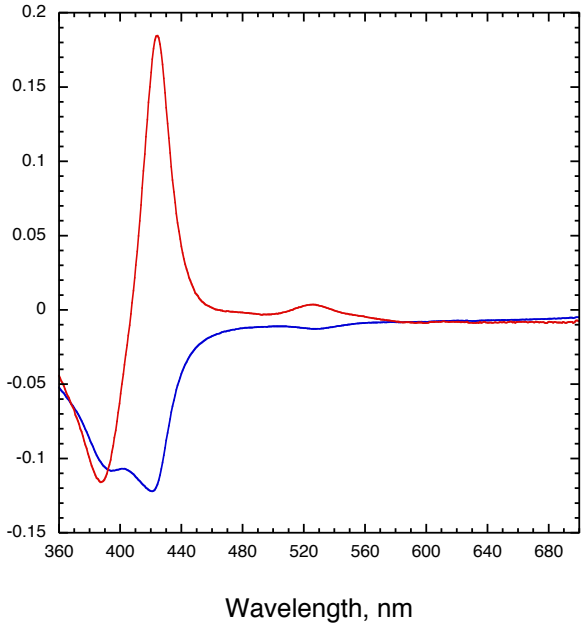

Figure S23. Abstract spectra resulting from the SVD analysis of the titration results for FeTDPS-II from Figure S9. Only two significant non-zero singular values were obtained from SVD analysis.

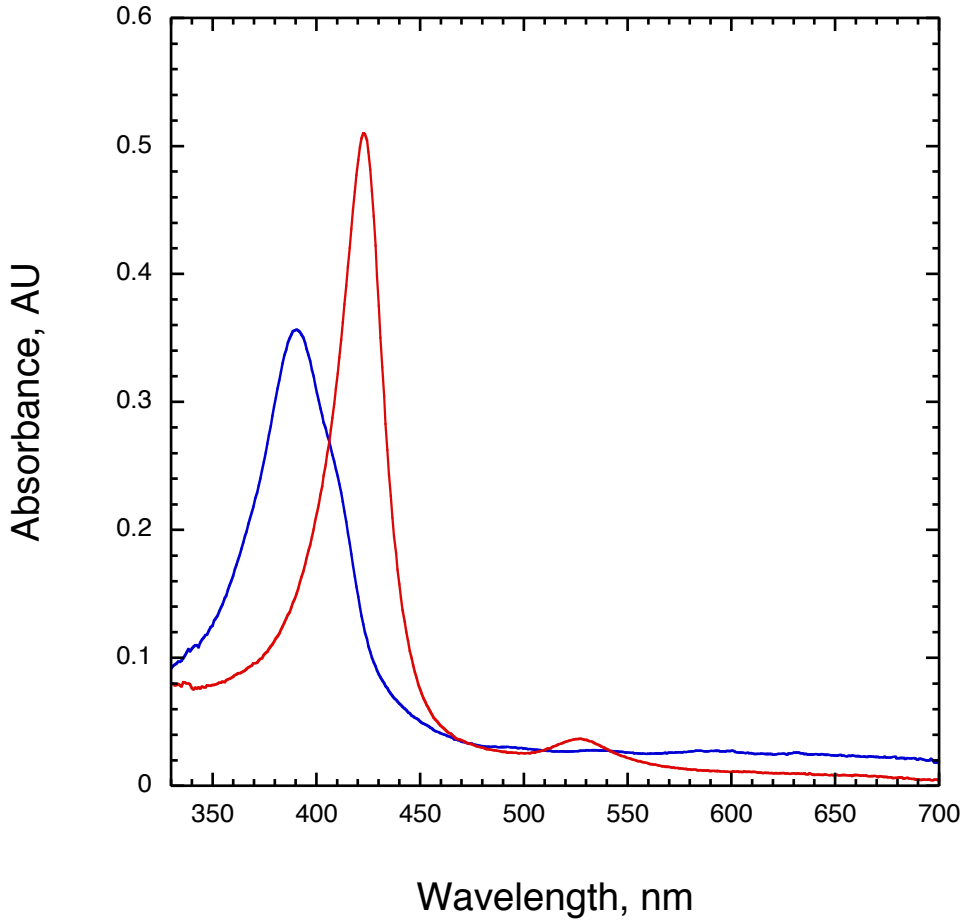

Figure S24. FeTDPS-II electromer spectra reproduced using model free evolving factor analysis (EFA) of the titration data in Figure S9.

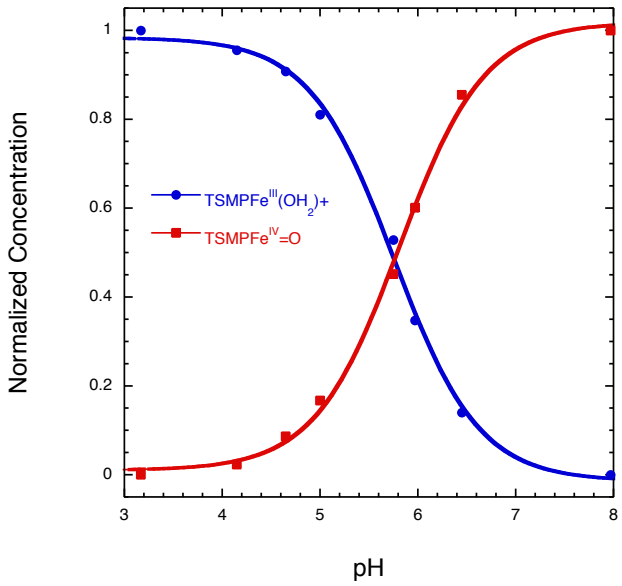

Figure S25. Concentration profile for the two observed electromers of FeTSMP-II as determined by model free evolving factor analysis (EFA) of the titration data shown in Figure S10. The observed pK_a^{obs} values determined by fitting the SVD speciation data are 5.76 $\pm$ 0.04 ($TSMPFe^{III}(OH_2)_2$ fit) and 5.81 $\pm$ 0.04 ($TSMPFe^{IV}$=O fit), dx = 0.36 $\pm$ 0.03.

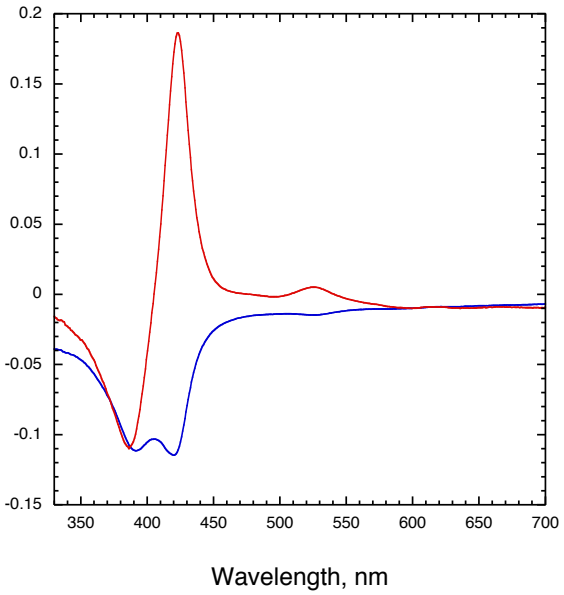

Figure S26. Abstract spectra resulting from the SVD analysis of the titration results for FeTSMP-II in Figure S10. Only two significant non-zero singular values were obtained from SVD analysis.

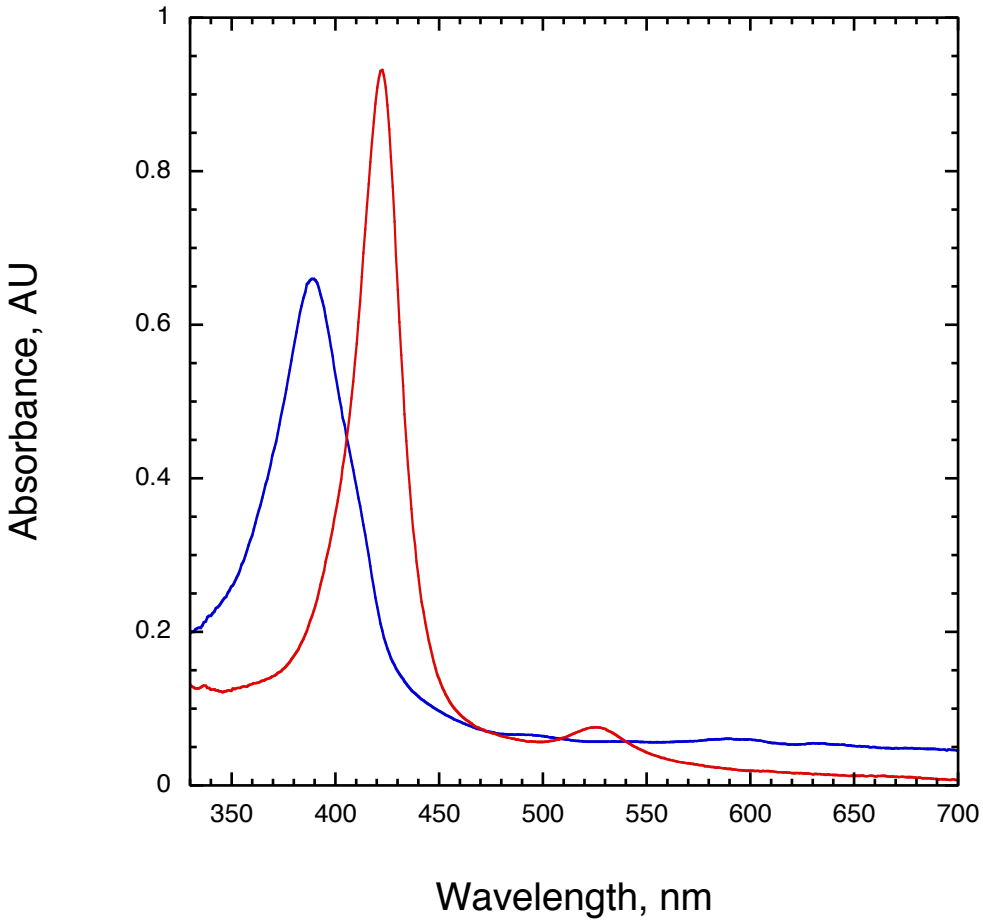

Figure S27. FeTSMP-II electromer spectra reproduced using model free evolving factor analysis (EFA) of the titration data.

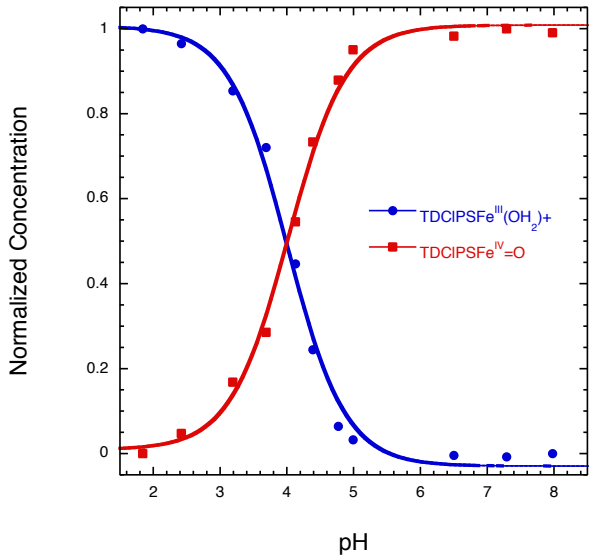

Figure S28. Concentration profile for the two observed electromers of FeTDClPS II as determined by model free evolving factor analysis (EFA) of the titration data shown in Figure S11. The observed pKa^{obs} determined by fitting the SVD speciation data are 4.01 ± 0.05 ($TDClPSFe^{III}(OH_2)_2$ fit) and 4.02 ± 0.04 (TDClPS Fe^{IV}=O fit), *dx* = 0.36 ± 0.03.

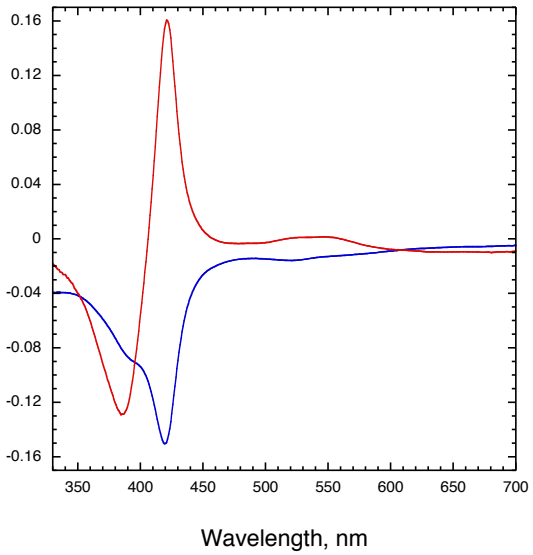

Figure S29. Abstract Spectra resulting from the SVD analysis of the titration results for FeTDClPS II which are shown in Figure S11. Only two significant non-zero singular values were obtained from SVD analysis.

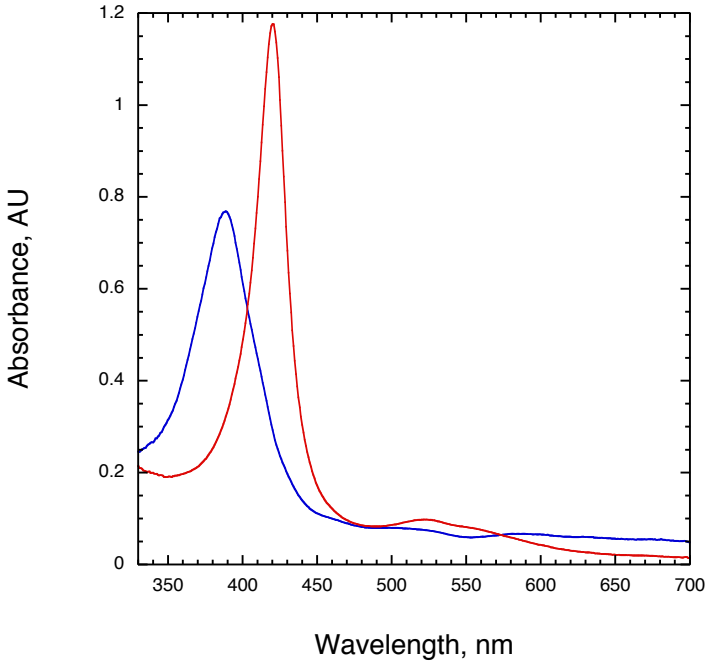

Figure S30. FeTDClPS-II electromer spectra reproduced using model free evolving factor analysis (EFA) of the titration data.

Derivation of equation 2 and calculation of $D(OH_2)$.

$D(OH_2) = -\Delta G_{Tot} = -(\Delta G_a + \Delta G_b)$

$D(OH_2) = -(\{ -23.06*E'_{Cpd\text{-}I} - 1.37*pK_a2 - 57 \} + \{ -1.37*pK_a1 + 1.37*pH \})$

$D(OH_2) = -(-23.06*E'_{Cpd\text{-}I} - 1.37*(pK_a2 + pK_a1) + 1.37*pH - 57)$, where $pK_a^{obs} = (pK_a2 + pK_a1) / 2$

$D(OH_2) = 23.06*E'_{Cpd\text{-}I} + 1.37*(2\ pK_a^{obs}) - 1.37*pH + 57$ (eq 2)

$D(OH_2)$ parameters were calculated using the following E' for P^+-Fe^{IV}=O/P-Fe^{IV}=O: FeTSMP 1.097 V; FeTDPS 1.025 V; FeTMPS 1.063 V; FeTDClPS 1.257 V vs NHE.

(FeTSMP) $D(OH_2)$ = 91.5 kcal/mol at pH 5.0

(FeTMPS) $D(OH_2)$ = 89.5 kcal/mol at pH 5.0

(FeTDPS) $D(OH_2)$ = 91 kcal/mol at pH 5.0

(FeTDClPS) $D(OH_2)$ = 90.5 kcal/mol at pH 5.0

References

1. Bell, S. R. Modeling Heme Monoxygenases with Water-Soluble Iron Porphyrins. PhD Thesis, Princeton University, Princeton, 2010.